Pertanika J. Sci. & Technol. 34 (3): 1309 - 1329 (2026)

PERTANIKA JOURNALS

SCIENCE & TECHNOLOGY

Journal homepage: http://www.pertanika.upm.edu.my/

Valorisation of Oil Palm Waste into Magnetic Catalysts for Efficient Synthesis of Bio-additive Ethyl Levulinate: Optimisation of Reaction Parameters

Shamala Gowri Krishnan[1] and Pua Fei Ling[2,3]*

[1]College of Graduate Studies, Universiti Tenaga Nasional, 43000 Kajang, Selangor, Malaysia
[2]Institute of Sustainable Energy (ISE), Universiti Tenaga Nasional, 43000 Kajang, Selangor, Malaysia
[3]Department of Mechanical Engineering, College of Engineering, Universiti Tenaga Nasional, 43000 Kajang, Selangor, Malaysia

ABSTRACT

Levulinate esters are promising value-added energy chemicals that have piqued researchers' worldwide interest owing to their potential as fuel additives. The reactions mainly concentrate on catalytic performance and offer limited research on the use of biomass-derived solid catalysts. This study investigated the efficiency of palm waste-derived magnetic solid catalysts and optimised the esterification process to improve ethyl levulinate yield. The results showed that the sulfonic group, $–SO_3H$, provides strong Brønsted acid sites for esterification, while ferric ions, Fe^{3+}, act as Lewis acids to enhance carbonyl activation, jointly catalysing the conversion to ethyl levulinate. The ethyl levulinate yield reached 87.0 mol%, achieved with an EFB fibre/γ-Fe_2O_3 catalyst (9.1 wt%) and an ethanol-to-levulinic acid molar ratio of 13.6:1 at 66.7 °C for 6 h. FT-IR and GC-FID analyses validated the formation of the ester groups following the esterification reaction. The catalyst can be easily removed with an external magnet, offering an effective way to use solid catalysts in esterification.

Keywords: Empty fruit bunch, ethyl levulinate, magnetic, mechanism, optimisation

ARTICLE INFO

Article history:
Received: 08 October 2025
Accepted: 18 March 2026
Published: 12 June 2026

DOI: https://doi.org/10.47836/pjst.34.3.02

E-mail addresses:
shamalagowri.k@gmail.com (Shamala Gowri Krishnan)
gracepua@uniten.edu.my (Pua Fei Ling)
* Corresponding author

INTRODUCTION

Interest in developing alternative fuels and chemicals from sustainable biomass has increased over the last decade, as climate change associated with using non-renewable fuels has been recognised globally (Gielen et al., 2019). Several alternatives are needed to reduce the world's dependence on

e-ISSN: 2231-8526

© Universiti Putra Malaysia Press

fossil fuels, particularly in transportation. Compared to fossil fuels, biodiesel has a lower environmental impact as it is produced from renewable feedstocks. Biodiesel in larger quantities is severely hampered by its higher density, lower calorific value, poor oxidation stability, higher nitrogen oxide emissions and poor cold flow properties (Martínez Aguilar et al., 2020). Biodiesel, when combined with fuel additives, can address these problems by improving diesel engine efficiency and reducing emissions. There are various additives, such as metal-based additives, oxygenates, and antioxidants. Ethyl levulinate, synthesised from levulinic acid, has been recommended as an effective oxygenate additive.

Levulinic acid (LA), chemically known as 4-oxopentanoic acid, gamma-ketovaleric acid or 3-acetylpropionic acid, is a linear C5 alkyl carbon chain and is considered one of the twelve most promising biomass-derived chemicals (Signoretto et al., 2019). Ester derivatives of levulinic acid are commonly used as flavouring agents, in fragrances, pharmaceutical intermediates, and as fuel additives. Alkyl levulinates are an appealing substance because they can be used up to 5 wt% as a miscible biofuel in diesel engines (Enumula et al., 2017). There are four methods for the synthesis of levulinate esters: one-pot synthesis, catalytic alcoholysis of furfural, reduction of furfural to furfuryl alcohol, and then catalytic alcoholysis and direct esterification using solid acid catalysts (Adeleye et al., 2019). All these methods have their advantages and disadvantages. However, direct esterification is the simplest and most sustainable method, using various solid acid catalysts such as zeolites, silica, heteropolyacids, mixed-metal oxides, and nanostructured solid acids (Ogino et al., 2018). Previously, it was known that dilute sulphuric acid is economical and can provide sufficient protons (Bronsted acid) to catalyse the reaction. Due to difficulties in extraction and their corrosive nature, liquid catalysts were limited. Alkyl levulinates (ALs) can be prepared via esterification reactions using various alcohols, such as methanol, ethanol, and butanol (Yan et al., 2017). The most common ALs are methyl levulinate and ethyl levulinate. Methyl levulinate is a short-chain ester with comparable properties to fatty acid methyl ester (FAME) (Liu et al., 2020). It can be utilised as a biodiesel additive owing to the following characteristics: (i) high lubricity, (ii) non-toxicity, and (iii) enhanced cold flow properties. Ethyl levulinate (EL) is one of the most potent fuel additives. Its sulphur-free nature has shown great promise for petrol blends and diesel engines. Furthermore, it is utilised as a flavouring agent, a fuel-oxygenate additive, and a precursor to various chemicals that can be converted into fuels. Among these ALs, ethyl levulinate is the most promising due to its compatibility with both petroleum and biodiesel and its potential as a future fuel substitute.

Although alcoholysis is efficient with liquid catalysts, its use has significant drawbacks, including difficulty in acid recovery, equipment degradation, and environmental pollution. Furthermore, corrosive environments require special materials for reactor construction, increasing capital and operating costs. These drawbacks can be addressed by substituting

liquid acid catalysts with solid catalysts. Solid catalysts offer many advantages, including easy recovery from reaction products, recyclability, and reduced susceptibility to corrosion. As a result, many solid acid catalysts have been widely used in esterification processes. Zhou et al. (2025) prepared a titanium dioxide nanotube-based solid acid catalyst (TNTs-PhSO_3H) that achieved a maximum yield of 98% at a catalyst loading of 12 wt% (Zhou et al., 2025). Costa et al. (2024) synthesised alkyl levulinate using mesoporous Stann silicates, achieving a maximum yield of 83.6% at a catalyst loading of 1 wt% and a reaction temperature of 120 °C (Costa et al., 2024). However, in the process, acidic ion-exchange resins, zeolites, silica, and heteropoly acid-based catalysts were primarily used to esterify levulinic acid (Zhao et al., 2020). Due to environmental concerns, solid biomass-based catalysts could be a viable alternative to current solid catalysts. Campana et al. (2023) synthesised heterogeneous acid catalysts using pine needles as a carbon source and found that sulfonated pine needles (PiNe-SO_3H) had the highest levulinate yield of 93% (Campana et al., 2023). Meanwhile, Saperi et al. (2024) reported that esterification of LA using lignin-based acid catalyst showed the maximum conversion of ethyl levulinate (EL) with 62.5 % at 80 ^oC after 3 h of reaction with 10 wt% catalyst loading (Saperi et al., 2024). The author also tested with acidic DES, which acts as a co-catalyst, further enhancing the yield to 81.7%. Besides, Patel and Rave (2025) worked on a sugarcane bagasse-based solid acid catalyst for the synthesis of biofuel additives. They reported that a 53 % conversion of levulinic acid and a 93 % selectivity for n-butyl levulinate were achieved under relatively mild conditions, such as a 1:2 molar ratio of acid to alcohol, 25 mg catalyst, 8 h, and 90 °C (Patel & Dave, 2025). Regardless of the type of carbon source used, there are no reports of using EFB or its derivatives in catalyst synthesis for producing levulinate ester.

This study investigates the synthesis of ethyl levulinate using magnetic solid catalysts based on empty fruit bunch (EFB) and explores the mechanism behind the catalyst's performance in the esterification reaction. A parametric study identified the optimal conditions for the esterification process. The effects of catalyst loading, ethanol-to-LA molar ratio, processing time, and temperature on esterification over magnetic solid catalysts were studied using the Box-Behnken design. Additionally, a reaction mechanism study highlighted the advantages of biomass-derived magnetic acid catalysts to produce bio additives.

MATERIALS AND METHODS

Materials

Analytical reagents, Levulinic acid (99%), were purchased from Merck, and Ethanol, 95% (Dulab), was bought from Suria Pembekal Umum Sdn. Bhd, Malaysia.

Synthesis of Ethyl Levulinate

The esterification reaction was carried out using EFB fibre/γ-Fe_2O_3, EFB lignin-SO_3H-Fe_3O_4, and EFB MCC/γ-Fe_2O_3, (Krishnan et al., 2020; Krishnan et al., 2022) along with a blank experiment as a control. The catalyst preparation methods were summarised in Table 1. The esterification of levulinic acid (LA) with ethanol, using magnetic solid catalysts derived from EFB, was carried out in a reflux setup. 10 g of levulinic acid and ethanol at a 10:1 molar ratio was heated to 70 °C. Once the target temperature was reached, 10 wt% of the prepared catalyst was added, and the mixture was stirred for 5 h. After the reaction, the catalyst was removed using a magnet and the excess ethanol was evaporated at 80 °C. The yield (EL_C) was calculated using Equation 1.

$$EL_C = \left(\frac{EL_n}{LA_n}\right) \times 100 \quad [1]$$

where EL_n is the mole of EL formed, and LAn is the initial mole of LA.

Table 1
The summary of catalysts preparation and their characteristics

Catalyst Type	Raw Material	Preparation Method	Characteristics (i; ii; iii; iv)
EFB fibre/γ-Fe_2O_3	Treated EFB fibre	Co-precipitation and Calcination	37.9 (C), 34.8 (O), 21.8 (Fe), 5.5 (S); 2.4 mmol/g; 188.87 m^2/g, 11.5 nm; 24.97 emu/g
EFB lignin-SO_3H-Fe_3O_4	Lignin (extracted from EFB)	Hydrothermal Carbonisation, Calcination and Sulfonation	52.7 (C), 25.0 (O), 17.5 (Fe), 4.8 (S); 2.2 mmol/g; 56.88 m^2/g, 4.8 nm; 21.78 emu/g
EFB MCC /γ-Fe_2O_3	Microcrystalline cellulose (extracted from EFB)	Co-precipitation and Calcination	42.9 (C), 18.2 (O), 26.9 (Fe), 11.9 (S); 2.5 mmol/g; 290.55 m^2/g, 3.5 nm; 21.27 emu/g

Note. i-elemental results; ii-acidity; iii-surface area and pore size; iv-magnetism. Adapted from, (Krishnan et al., 2020; Krishnan et al., 2022)

Fourier Transform Infrared Analysis

The functional group in the esterified samples was identified using a Shimadzu IR Prestige-21 FT-IR spectrophotometer at Universiti Tenaga Nasional, UNITEN. Spectra were recorded over the 4000-400 cm^{-1} range. A small sample was placed on a KBr plate and covered with another to form a thin film. This film was then positioned in the sample holder, and the spectrum was recorded to analyse the carboxyl group based on its functional group.

Box-Behnken Optimisation of Esterification Reaction Parameters

The response surface methodology, specifically the Box-Behnken approach, was employed to optimise four independent variables: catalyst loading (A), ethanol-to-LA molar ratio (B), reaction time (C), and reaction temperature (D). The range of variables was determined by the literature review and initial experiments conducted (Nelson Appaturi et al., 2022; Trombettoni et al., 2017). The range of experimental values used is as follows: 5-15 wt% catalyst loading, 5:1-15:1 molar ratio of ethanol-to-LA, 3-7 h and 65-75 °C. The experimental data used to optimise the esterification reaction were obtained from Design-Expert, with the conversion rate serving as the response variable. The results of the randomised experimental runs were correlated with the variables via a full quadratic model, Equation 2.

$$Y = \beta_0 + \sum_{i=1}^{4} \beta_i x_i + \sum_{i=1}^{4} \beta_{ii} x_i^2 + \sum_{i=1}^{3} \sum_{j=i+1}^{4} \beta_{ij} x_{ij} \quad [2]$$

where Y represents the response (in percentage), βo is the intercept's regression coefficient, βi is the coefficient for the linear term, βii is the coefficient for the quadratic term, and βij is the coefficient for the interaction term, xi and xij are independent variables, and ε denotes the error.

The independent variables and their ranges used in the optimisation are shown in Table 2. The esterification reaction was carried out under reflux, using LA. The catalytic performance of the most effective magnetic acid catalyst was assessed. Table 3 displays the Box-Behnken experimental design.

Gas Chromatography-Flame Ionisation Detector Analysis

The ethyl levulinate yield was determined by GC (Agilent Technology, 7890A) using a capillary column from DB-WAX (30 m x 0.32 mm x 0.25 µm). The prepared ester samples (1 g) were dissolved in 10 mL of heptane for analysis. The column temperature was 220 °C, while the injector and detector (FID) temperatures were 250 °C and 280 °C, respectively. The yield percentage was determined from the standard EL concentration using the calibration curve and calculated using the following equation Equation 3. The peaks of ethyl levulinate were identified by comparing their retention times with those of the standards.

$$EL_y = \left(\frac{\left(\left(\frac{(C_E \times V_P)}{1000} \right) / M_E \right)}{\left(\frac{W_i}{M_L} \right)} \right) \times 100 \quad [3]$$

where EL_y is EL yield (mol%), C_E is the concentration of LE (mg/ml), M_E and M_L are the MM of EL and LA (g/mol), respectively, V_p is the final volume of the product (mL), and W_i is the weight of LA (g).

Table 2
The variables and ranges for the optimisation study

Variables	Symbol	-1	0	+1
Catalyst (%)	A	5	10	15
Ethanol-to-LA (molar ratio)	B	5:1	10:1	15:1
Time (h)	C	3	5	7
Temperature (^oC)	D	65	70	75

Table 3
Box-Behnken design of the experiment for optimisation study

Run	Catalyst, %	Ethanol: LA	Time, h	Temperature, ^oC
1	10	10:1	7	65
2	15	10:1	5	75
3	15	5:1	5	70
4	5	15:1	5	70
5	5	10:1	5	75
6	10	15:1	3	70
7	10	15:1	5	75
8	5	10:1	3	70
9	10	5:1	5	65
10	10	5:1	5	75
11	10	5:1	3	70
12	5	5:1	5	70
13	10	5:1	7	70
14	10	15:1	7	70
15	10	10:1	7	75
16	10	10:1	5	70
17	10	10:1	3	65
18	5	10:1	5	65
19	10	10:1	3	75
20	10	15:1	5	65
21	15	10:1	3	70
22	15	15:1	5	70
23	5	10:1	7	70
24	15	10:1	5	65
25	15	10:1	7	70

Catalyst Reusability

The reusability study was carried out using the optimised parameters to assess the catalyst's reusability. After each cycle, the catalyst was recovered using a magnet, washed with ethanol until the filtrate was neutral, and dried in an oven at 60 °C overnight for future reactions, without further removal or activation.

RESULTS AND DISCUSSIONS

Effect of EFB-derived Magnetic Catalysts on Ethyl Levulinate Yield

The efficiency of catalysts- EFB fibre/γ-Fe_2O_3, EFB lignin-SO_3H-Fe_3O_4, and EFB MCC/γ-Fe_2O_3- in esterifying levulinic acid was tested using ethanol as the primary alcohol. The reaction was performed using 10 wt% catalyst and an ethanol-to-LA molar ratio of 10:1 at 70 °C for 5 h. Ethyl levulinate levels were analysed using a GC-FID. Figure 1 shows the conversion of LA to EL, with a control experiment (no catalyst) showing only 0.95 mol% conversion. Catalysts significantly improved yields, highlighting the importance of the acid catalyst. The highest yield reached 84.87 mol% with an EFB fibre/γ-Fe_2O_3 catalyst. Yields for EFB lignin-SO_3H-Fe_3O_4 and EFB MCC/γ-Fe_2O_3 catalysts were 80.58 mol% and 74.06 mol%, respectively. Based on FT-IR analysis (Krishnan et al., 2020; Krishnan et al., 2022), oxygen-containing functional groups, such as -SO_3H, -O-, -OH and C=O, were present in both the EFB fibre/γ-Fe_2O_3 and EFB lignin-SO_3H-Fe_3O_4 catalysts, leading to ethyl levulinate yields exceeding 80 mol%. Additionally, the EFB fibre has a wide variety of accessible oxygenated groups (from cellulose, hemicellulose, and lignin), which provide more reactive sites (Krishnan et al., 2023), and EFB lignin has many oxygen groups but is less accessible, thus reducing the yield. On the other hand, EFB MCC has hydroxyl (-OH) groups but fewer diverse oxygen functionalities, which limit conversion.

Compared with other studies on the production of EL using solid acid catalysts, EFB fibre/γ-Fe_2O_3 yields a higher ethyl levulinate yield. Li et al. (2019) achieved excellent catalytic activity for producing ethyl levulinate from carbonic acid using a loofah sponge, with a maximum yield of 91%, but the reaction required 12 h at 80 °C (Li et al., 2019). Catalysts with higher –SO_3H content provide more Brønsted acid sites, which enhance protonation of the levulinic acid carbonyl group, thereby accelerating esterification. In addition, oxygen-containing groups (-OH and C-O) enhance the adsorption of reactants and facilitate interactions with Fe active sites. In this case, EFB fibre/γ-Fe_2O_3 catalyst, which possesses a higher diversity and accessibility of oxygen functionalities, exhibited the highest EL yield.

Chemical Analysis

FT-IR analysis was conducted to confirm the presence of ester groups in the esterified products. Figure 2 displays the FT-IR spectra of the esterified samples prepared with EFB-derived magnetic acid catalysts, alongside a blank sample. A control experiment assessed the catalysts' effectiveness in converting LA. The findings indicate that all esterified samples exhibit peaks identical to those in the control.

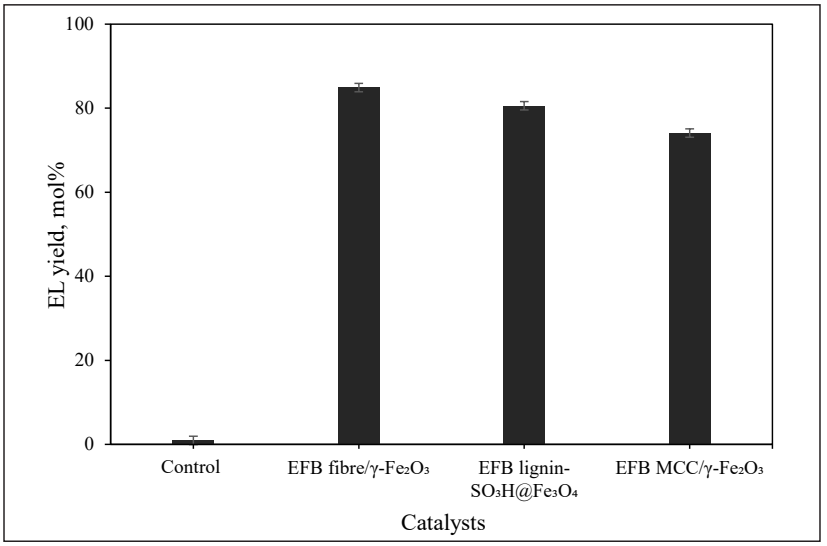

Figure 1. Ethyl levulinate yield using EFB-based magnetic solid catalysts and a blank experiment

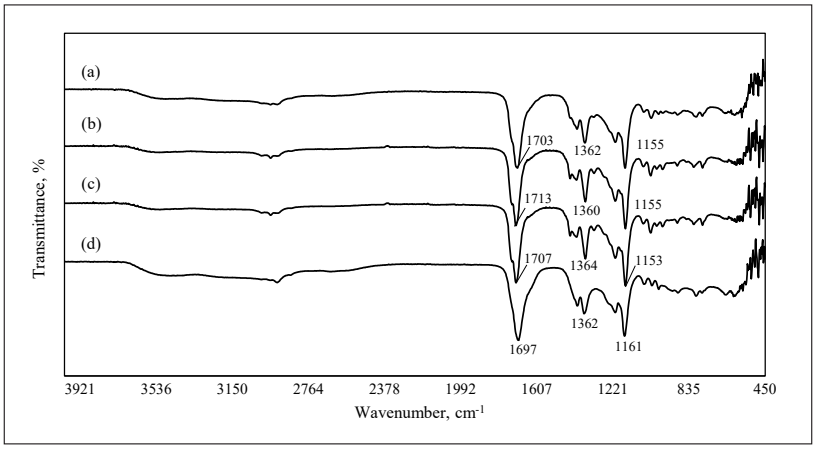

Figure 2. FT-IR spectra of esterified levulinic acid using (a) EFB fibre/γ-Fe_2O_3; (b) EFB lignin-SO_3H-Fe_3O_4; (c) EFB MCC/γ-Fe_2O_3; and (d) control experiment

The sharp absorption bands observed in 1703, 1709, and 1713 cm^{-1} are attributed to the C=O stretching of the carbonyl group, suggesting the presence of aldehyde and ketone groups in these samples, with a closely similar peak at 1697 cm^{-1} in the control sample. Thus, they indicate the presence of esters in the samples (Faraguna et al., 2019). The absorption bands near 1360, 1362, and 1364 cm^{-1} correspond to alkyl C-H bending vibrations, indicating the presence of ethyl groups in the esterified samples. Additionally, bands at 1153, 1155, and 1161 cm^{-1} are associated with C–O stretching of the ester group, which may also be present in the levulinic acid. However, the IR spectra of the esterified samples and the blank sample were justified by the prior ethyl levulinate yield and GC-FID results (Figure S1 to S4) for these samples.

Statistical Analysis and 3D Surface Models via Box-Behnken

Based on the effect of EFB-derived magnetic acid catalysts, EFB fibre/γ-Fe_2O_3 exhibited good catalytic activity. Its efficiency in determining optimal reaction conditions was further investigated using a response surface methodology (RSM) optimisation study. The RSM model's optimum conditions denote the theoretical maximum within the studied parameter space. These conditions were experimentally confirmed, and the EL yield closely matched the predicted value, validating the model's accuracy. The best observed run corresponds to the highest yield among the experimental points, which might differ slightly from the predicted optimum because the model estimates the ideal conditions between discrete levels. A four-factor, three-level optimisation plan was developed employing the Box-Behnken model with the following parameters: catalyst (A), molar ratio of ethanol-to-LA (B), temperature (C), and time (D). A total of 29 experiments were conducted for LA esterification. Table 4 to 6 presents the experimental and predicted conversion results, the analysis of variance, and the statistical model analysis. Figure 3 illustrates the comparison between predicted and experimental (actual) data. The points scattered near the diagonal clearly show the relationship between the predicted and actual conversion rates. Analysis of variance (ANOVA) was used to test the statistical significance of the quadratic model and to evaluate interactions between the reaction parameters and the response.

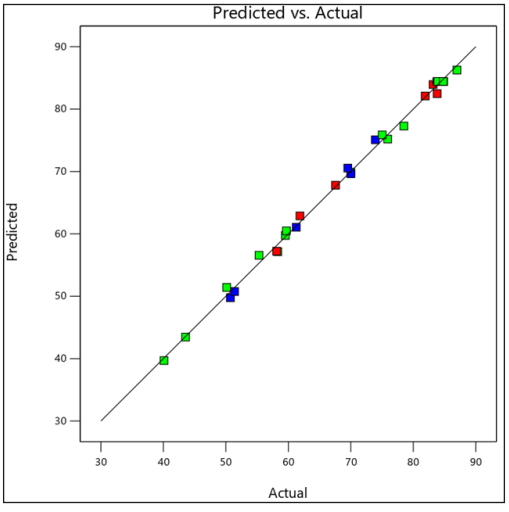

Figure 3. Comparison of actual versus predicted yield data

From the model analysis in Table 5, the larger F-value (304.55) and lower *p*-value (< 0.0001) indicate that the corresponding parameters are significant. Statistical analysis revealed that all parameters and interactions were significant. For the primary parameters, the molar ratio of ethanol-to-LA and reaction time were highly significant ($p < 0.0001$), followed by catalyst loading ($p = 0.0002$) and reaction temperature ($p = 0.0017$). For the interaction parameters, AB, AC, AD, and BC were statistically significant ($p < 0.05$), followed by BD ($p = 0.0085$) and least significant for CD ($p = 0.022$).

Table 4
Experimental results of the response surface analysis of ethyl levulinate yield

No.	Catalyst, %	Ethanol: LA Molar Ratio	Temperature, °C	Time, h	EL Yield, mol%	Predicted Yield, mol%
1	15	15:1	70	5	70.0	71.1
2	10	5:1	70	3	51.4	51.9
3	15	10:1	75	5	75.0	76.6
4	15	10:1	70	7	61.9	63.8
5	10	15:1	65	5	87.0	87.4
6	10	15:1	70	3	69.5	70.3
7	10	15:1	70	7	83.2	84.3
8	5	5:1	70	5	43.6	45.6
9	5	10:1	70	3	50.7	52.0
10	5	15:1	70	5	59.5	61.6
11	10	10:1	70	5	83.8	83.9
12	10	10:1	70	5	83.9	83.9
13	10	5:1	70	7	58.1	57.9
14	10	10:1	75	3	70.0	70.3
15	10	5:1	75	5	59.7	60.0
16	10	10:1	75	7	83.8	84.3
17	10	5:1	65	5	55.3	57.0
18	10	10:1	65	3	73.9	75.3
19	15	5:1	70	5	40.1	41.2
20	5	10:1	75	5	50.1	51.4
21	15	10:1	65	5	58.3	57.9
22	5	10:1	65	5	75.9	77.1
23	10	10:1	65	7	81.9	82.8
24	15	10:1	70	3	61.3	62.0
25	10	10:1	70	5	84.9	84.9
26	5	10:1	70	7	67.6	68.9
27	10	10:1	70	5	84.8	84.8
28	10	10:1	70	5	84.8	84.8
29	10	15:1	75	5	78.5	81.7

Table 5
ANOVA for the quadratic model

	Sum of Squares	df	Mean Square	F Value	P-value	
Model	5471.80	14	390.84	304.55	< 0.0001	significant
A-Catalyst	30.62	1	30.62	23.86	0.0002	
B-Ethanol: LA molar ratio	1621.69	1	1621.69	1263.66	< 0.0001	
C-Temperature	19.20	1	19.20	14.96	0.0017	
D-Time	295.72	1	295.72	230.43	< 0.0001	
AB	48.44	1	48.44	37.75	< 0.0001	
AC	451.35	1	451.35	351.70	< 0.0001	
AD	65.77	1	65.77	51.25	< 0.0001	
BC	41.54	1	41.54	32.37	< 0.0001	
BD	12.01	1	12.01	9.36	0.0085	
CD	8.47	1	8.47	6.60	0.0223	
A^2	2157.53	1	2157.53	1681.20	< 0.0001	
B^2	1095.64	1	1095.64	853.75	< 0.0001	
C^2	10.78	1	10.78	8.40	0.0117	
D^2	219.74	1	219.74	171.23	< 0.0001	
Residual	17.97	14	1.28			
Lack of Fit	16.82	10	1.68	5.88	0.0513	not significant
Pure Error	1.15	4	0.29			
Cor Total	5489.76	28				

Based on the quadratic terms, the significant trend was $A^2 > B^2 > D^2 > C^2$. Therefore, the statistical analysis indicates that the parameters with the most significant impact on ethyl levulinate yield were catalyst loading, molar ratio of ethanol-to-LA, and reaction time. Conversely, the reaction temperature had a lesser effect on yield, although it remains crucial for the model. Referring to Table 4, the equation with coded variables is used to describe the reaction parameters in Equation 4.

$$Y = 84.4 + 1.6\mathrm{A} + 11.6\mathrm{B} - 1.3\mathrm{C} + 4.9\mathrm{D} + 3.5\mathrm{AB} + 10.6\mathrm{AC} - 4.1\mathrm{AD} - 3.2\mathrm{BC} + 1.7\mathrm{BD} + 1.5\mathrm{CD} - 18.2A^2 - 12.9B^2 - 1.3C^2 - 5.8D^2 \quad [4]$$

where A, B, C, and D are the values of the catalyst, ethanol-to-LA molar ratio, temperature, and time, respectively, and Y is the response of the EL yield.

A, B, and D were the most important parameters for achieving higher ethyl levulinate yields in the esterification reaction. According to Table 4, the highest ethyl levulinate yield of 87.0 mol% was obtained under optimal reaction conditions: 10 wt% catalyst loading,

a molar ratio of 15:1 ethanol-to-LA, and 65 °C for 5 h. The statistical analysis of the regression coefficient of the model was carried out using the determination R^2 value, which was 1.00, indicating that the quadratic model Equation 4 predicts 100% of the initial reaction and is highly reliable. Table 6 shows that the adjusted R^2 of 0.99 is close to the predicted R^2 of 0.98. It can be assumed that the model fits well, as the coefficient of variation (C.V.) is 1.65%, which is less than 10%. The regression model thus confirms that ethyl levulinate can be produced from levulinic acid via esterification. According to the Box-Behnken validation, the highest conversion rate of 87.1 mol% was achieved with a catalyst loading of 9.1 wt%, an ethanol-to-LA molar ratio of 13.6:1, at 66.7 °C for 6 h. The regression equation of this model follows the above test approach and is adaptable.

The relationship between the reaction parameters was shown by plotting two independent variables against the yield. The 3D model plots of the surface regression for yield are shown in Figure 4a-f. Figure 4a shows the interaction between the catalyst loading and the molar ratio of ethanol-to-LA at a constant time and temperature of 5 h and 70 °C on LA conversion in the 3D surface regression.

Table 6
Statistical analysis of the regression coefficient

Terms	Coefficient	Standard Error	t-Stat
Intercept	84.43	0.51	85.52
A-Catalyst	1.60	0.33	2.30
B-Ethanol: LA molar ratio	11.63	0.33	12.33
C-Temperature	-1.27	0.33	-0.56
D-Time	4.96	0.33	5.67
AB	3.48	0.57	4.69
AC	10.62	0.57	11.84
AD	-4.06	0.57	-2.84
BC	-3.22	0.57	-2.01
BD	1.73	0.57	2.95
CD	1.46	0.57	2.67
A^2	-18.24	0.44	-17.28
B^2	-13.00	0.44	-12.04
C^2	-1.29	0.44	-0.34
D^2	-5.82	0.44	-4.87
Statistical parameters	Values	Statistical parameters	Values
Standard deviation	1.13	R^2	1.00
Mean	68.57	Adjusted R^2	0.99
C.V.%	1.65	Predicted R^2	0.98
PRESS	98.68	Adequate R^2	57.16

The highest esterification yield was obtained with a high catalyst loading and a high molar ratio of ethanol-to-LA. In contrast, a lower esterification yield of 40.1 mol% was observed at a catalyst loading of 15 wt% and an ethanol-to-LA molar ratio of 5:1, probably due to the higher catalyst loading and the limited amount of ethanol used to facilitate the reaction. At lower catalyst loadings, the esterification yield was less than 60 mol% due to reduced contact between the active sites and the reaction reactants. The interaction term between catalyst loading and the molar ratio of ethanol-to-LA (F value 37.75) shows that it moderately influences the yield. Thus, the esterification yield with 10 wt% catalyst loading and a 10:1 molar ratio of ethanol-to-LA was 84.8 mol%.

Figure 4b illustrates the relationship between catalyst loading and reaction temperature in the 3D surface response model for EL preparation, maintained at constant time and ethanol-to-LA of 5 h and 10:1, respectively. Increasing the catalyst loading from 5 wt% to 10 wt% and raising the temperature from 65 to 70 °C led to a higher yield. However, at the lower catalyst loading (5 wt%) and higher reaction temperature (75 ^{o}C), the lowest yield of 50.1 mol% was observed, whereas at 15 wt% catalyst loading and 65 ^{o}C, the yield was 58.3 mol%. This is because, at lower catalyst loading, only a limited number of active sites are available for reaction. The addition of the catalyst to the reaction no longer has a significant effect once the maximum conditions are reached (Nindya et al., 2020). Furthermore, at higher reaction temperatures, the diffusion of reactants to the catalyst's active site increases. However, the large size of the reaction molecules (bulky intermediates) and the small pore size of the catalyst (as shown in Table 1) could reduce diffusion, preventing an increase in conversion rate. This indicates that the yield was low at extreme catalyst loadings and reaction temperatures, suggesting particle agglomeration and formation of larger intermediates, which deactivate the catalysts and block access to the active sites. The highest yield of 84.9 mol% was achieved with a 10 wt% catalyst loading at 70 °C.

Figure 4c presents a response surface plot of the relationship between catalyst loading and reaction time, with a constant ethanol-to-LA molar ratio of 10:1 and temperature at 70 °C. A high yield was discovered with moderate catalyst loading and reaction duration. The active sites enabled the reactants to react at a specific time, resulting in a high esterification yield. However, the yield decreased with decreasing catalyst loading at both shorter and longer reaction times. It could be due to the reaction mixture containing an excessive amount of catalyst at the shorter reaction time and a limited number of active sites at the longer reaction time (Zhang et al., 2019). Furthermore, increasing the catalyst loading reduced the conversion to 61.3 mol% due to inadequate interaction between the excess catalyst at a shorter reaction time of 3 h. At higher catalyst loadings, agglomeration of catalyst particles and increased diffusion resistance restrict access to –SO_3H and Fe active sites, thereby decreasing effective reactant-catalyst interactions and reducing the

esterification conversion. The maximum yield was 84.9 mol% with a 10 wt% catalyst loading for 5 h.

Figure 4d shows how the ethanol-to-LA molar ratio and reaction temperature interact to affect the yield, with a fixed catalyst loading of 10 wt% and a reaction time of 5 h. It suggests that the low accessibility of the catalyst surface, as the alcohol concentration decreased, led to a limited esterification process (Peng et al., 2014). At 65 °C, a lower yield of 55.3 mol% was obtained with a 5:1 ethanol-to-LA molar ratio. Despite this, a 15:1 ethanol-to-LA molar ratio at 65 °C significantly improved LA conversion to 87.0 mol%. As a result, increasing the molar ratio improved the yield by allowing better contact with the catalyst and exposing the active sites, thereby accelerating the process (compared to others). Research showed that a higher ethanol-to-LA molar ratio shifts the reaction equilibrium towards ethyl levulinate formation, suppresses the reverse hydrolysis by diluting the water, and improves solvation, while the increased temperature (65 °C) enhances the reaction and yields a higher EL (Sušjenka et al., 2024; Zainol et al., 2021). According to Thangaraj et al. (2019), acid catalysts yield well, but the reaction rate is sluggish, necessitating a higher alcohol-to-molar ratio to improve the reaction (Thangaraj et al., 2019). Kothe et al. (2020) found that an ethanol-to-LA molar ratio of 9:1 produced highly selective ethyl levulinate with up to 80% selectivity (Kothe et al., 2020). The interaction between the ethanol-to-LA molar ratio and reaction temperature revealed that both factors significantly affect the yield. As a result, at the maximum ethanol-to-LA molar ratio and moderate reaction temperature, a greater yield was attained.

Figure 4e shows the interaction between the ethanol-to-LA molar ratio and reaction time on the conversion of LA. When catalyst loading and reaction temperature were held constant at 10 wt% and 70 °C, respectively, the 3D surface model revealed that a moderate ethanol-to-LA molar ratio and a reaction temperature of 70 °C yielded higher conversion, ranging from 83.8 to 84.9 mol%. The conversion of LA was lower at a lower ethanol-to-LA molar ratio and a reaction time of 5:1 and 3 h, respectively. This is due to the limited amount of ethanol, as further adding ethanol might improve the yield (Nandiwale et al., 2013). However, increasing the ethanol-to-LA molar ratio and reaction time does not affect LA conversion because more ethanol dilutes the reactants, thereby limiting the conversion rate (Gautam et al., 2022). As a result, the maximum yield of 84.9 mol% was obtained at a 10:1 ethanol-to-LA molar ratio and a reaction time of 5 h. The result indicates that the catalyst achieves a high yield under moderate conditions.

The interaction between reaction temperature and duration does not influence the esterification of LA, as demonstrated in Figure 4f. The yield decreased as the interaction increased. At 70 °C and a 5 h reaction period, the most significant yield of 84.9 mol% was recorded. Furthermore, increasing the parameter value has no discernible influence on yield, with a slight decrease to 83.8 mol% after 7 h at 75 °C.

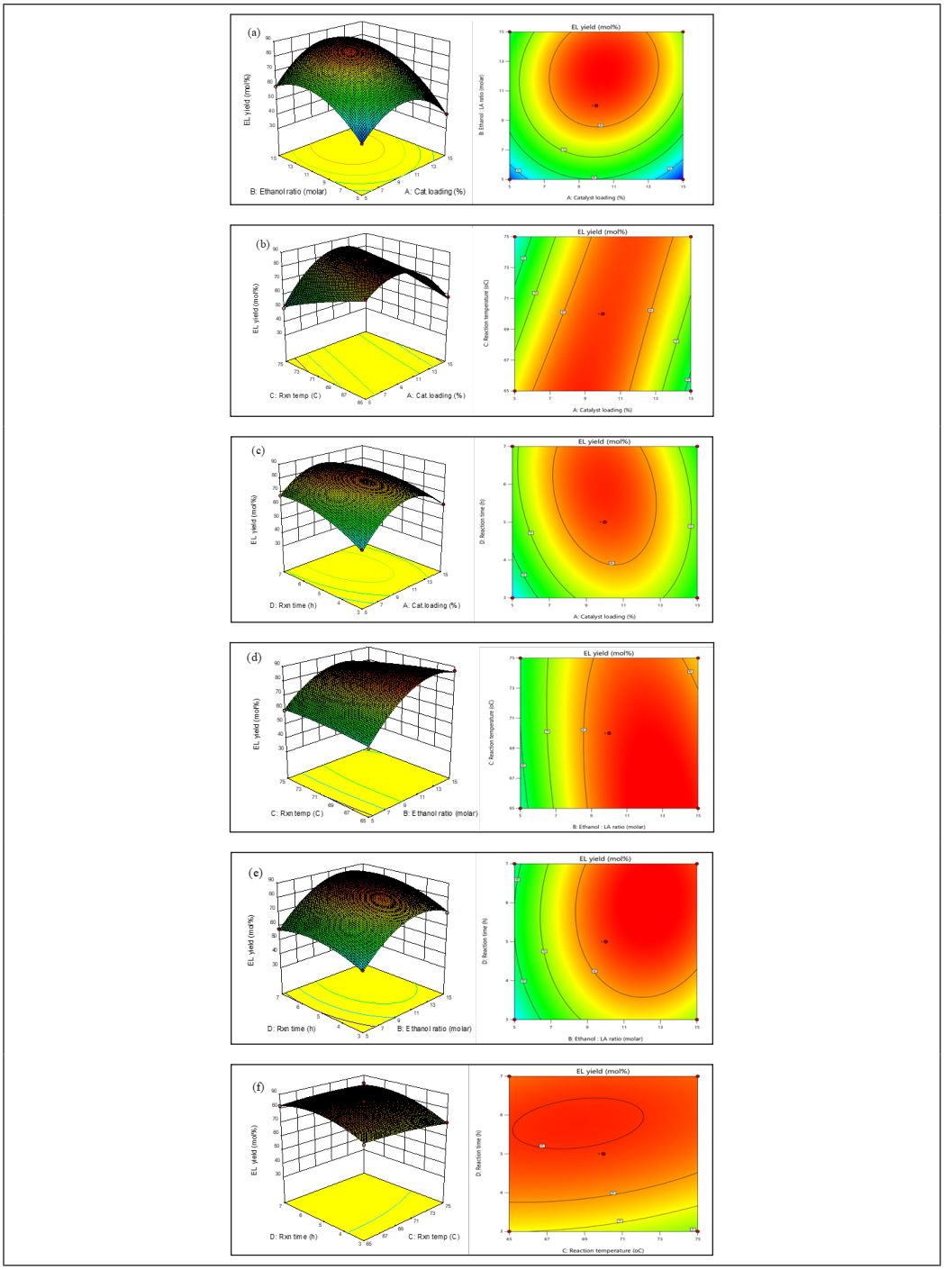

Figure 4. Surface regression 3D model plots and contour plots on ethyl levulinate yield with the interaction between (a) catalyst loading (wt%) and ethanol-to-LA molar ratio; (b) catalyst loading (wt%) and reaction temperature (°C); (c) catalyst loading (wt%) and reaction time (h); (d) ethanol-to-LA molar ratio and reaction temperature (°C); (e) reaction time (h) and ethanol-to-LA molar ratio; and (f) reaction temperature (°C) and reaction time (h)

However, the lowest yield of 70.0 mol% was observed after 3 h at 75 °C with minimal decrease. As a result, the interplay between reaction temperature and time has little effect on LA esterification. Kumaravel et al. (2019) found that LA conversion increased with increasing reaction temperature but did not show a significant yield (Kumaravel et al., 2019). Wang et al. (2020) found that reaction time does not substantially affect yield, and that the yield remains stationary before dropping (Wang et al., 2020). The analysis showed that the maximum yield of 87.0 mol% was achieved using the EFB fibre/γ-Fe_2O_3 with 9.1 wt% catalyst loading and 13.6:1 ethanol-to-LA molar ratio at 66.7 °C for 6 h.

Recyclability Study of EFB fibre/γ-Fe_2O_3 Catalyst

In industrial applications, catalyst stability is critical, and recyclability is essential in heterogeneous catalysis. Catalyst stability is repeatedly evaluated over several cycles. Figure 5 represents the EFB fibre/γ-Fe_2O_3 catalyst reusability for six cycles. According to the findings, the conversion of LA reduced from 87.0 mol% to 83.4 mol% after the second use and to 78.5 mol% after the fourth cycle. The catalyst activity remained steady after the 5th cycle, with only a slight decrease in LA conversion to 74.8 mol% after the sixth cycle. The decrease in the yield is most likely due to the leaching of active sites from the catalytic support by reactant contact (Trombettoni et al., 2018). However, further studies are necessary to definitively establish the reduction in catalytic yield. Furthermore, after 6 cycles, the catalytic activity of the EFB-derived magnetic acid catalyst did not decrease significantly, confirming its strong stability during LA esterification. The catalyst was reused without further regeneration to assess its stability and simulate practical process conditions where additional treatment steps are undesirable. This method shows the catalyst's ability to maintain activity with minimal processing. The gradual performance decline suggests that a mild regeneration step, such as thermal treatment, could restore active sites.

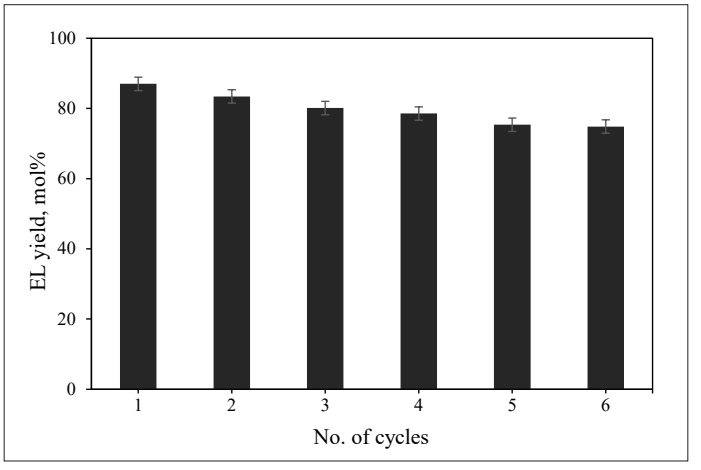

Figure 5. Recyclability of EFB fibre/γ-Fe_2O_3 for esterification of LA (optimised reaction parameters)

Mechanism of Catalytic Reaction

Figure 6 illustrates a possible reaction process of catalytic esterification of levulinic acid with ethanol in the presence of EFB fibre/γ-Fe_2O_3. FTIR analysis confirms the presence of –SO_3H groups, indicating Brønsted acid sites, while XRD patterns verify the formation of Fe-based phases (Fe-O), which can provide Lewis acidic centres. The coexistence of these functionalities suggests that both Brønsted and Lewis acid sites may contribute synergistically to the esterification reaction. Several steps are involved in the catalytic mechanism: (1) the first step consists of the acidic proton of the –SO_3H group interacting with the carbonyl oxygen of levulinic acid, forming protonated levulinic acid intermediates, (2) the protonation process enhances the electrophilic carbonyl carbon and the nucleophilic alcohol, and ethanol charges the carbonyl carbon to form oxonium ions (H_3O^+) (Guo et al., 2019); (3) the formed oxonium ions generate new sets of oxonium ions, leading to water loss of water; and (4) deprotonation proceeds to the formation of ethyl levulinate. The deprotonation process regenerates the acidic sites of the magnetic acid catalyst. Thus, using an acidic catalyst increases the esterification yield by catalysing the conversion of levulinic acid.

As for the Lewis acid sites, iron (Fe) is also responsible for the LA esterification reaction (Figure 7). In the first step, LA is directly coordinated with the surface of Fe^{3+} sites. In the following steps, the Lewis acid sites followed the same steps as the Bronsted acid, which catalysed the esterification reaction (Shestakova et al., 2021). The generation of oxonium ions corresponded to the acidity of the catalyst, and the presence of both Bronsted and Lewis acids aided in the conversion of LA to ethyl levulinate.

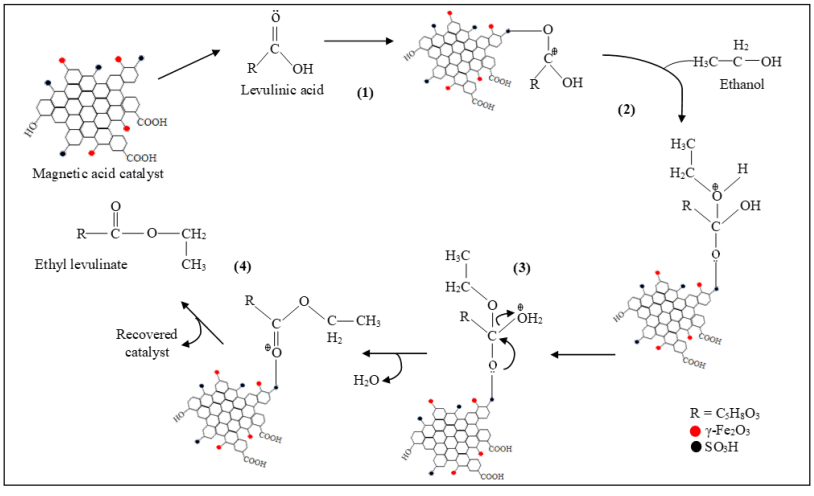

Figure 6. Proposed mechanism of Bronsted acid in the esterification of levulinic acid using EFB fibre/γ-Fe_2O_3 catalyst

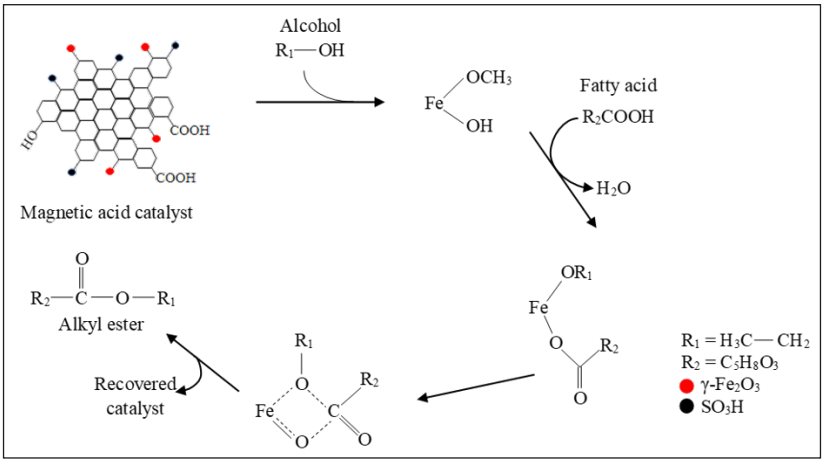

Figure 7. Proposed mechanism of Lewis acid in esterification reaction using EFB fibre/γ-Fe_2O_3 catalyst

CONCLUSION

The effectiveness of catalysts such as EFB fibre/γ-Fe_2O_3, EFB lignin-SO_3H-Fe_3O_4, and EFB MCC/γ-Fe_2O_3 in producing ethyl levulinate was evaluated. The EFB fibre/γ-Fe_2O_3 catalyst achieved the highest yield of 84.87 mol%, followed by EFB lignin-SO_3H-Fe_3O_4 with 80.58 mol%, and EFB MCC/γ-Fe_2O_3 with 74.06 mol%. A box-Behnken optimisation was conducted to assess the impact of reaction parameters on levulinic acid esterification. The maximum esterification yield of 87.0 mol% was obtained under optimised conditions with 9.1 wt% catalyst loading of EFB fibre/γ-Fe_2O_3, an ethanol-LA molar ratio of 13.6:1, at 66.7 °c, over 6 hours. Statistical analysis identified catalyst loading, ethanol-LA molar ratio, and reaction time as the most influential factors. This study emphasises the potential of biomass-based magnetic catalysts for sustainable chemical production, encouraging the utilisation of agricultural waste across various sectors and reducing landfill problems.

ACKNOWLEDGEMENT

This work was supported by the Dato' Low Tuck Kwong International Research Grant (20238024DLTK) and the Fundamental Research Grant Scheme (20180108FRGS). The authors also gratefully acknowledge the funding and facilities support provided by the UNITEN–AAIBE Project, Chair of Renewable Energy Grant (202303KETTHA).

REFERENCES

Adeleye, A. T., Louis, H., Akakuru, O. U., Joseph, I., Enudi, O. C., & Michael, D. P. (2019). A review on the conversion of levulinic acid and its esters to various useful chemicals. *AIMS Energy, 7*(2), 165-185. https://doi.org/10.3934/energy.2019.2.165

Campana, F., Valentini, F., Marrocchi, A., & Vaccaro, L. (2023). Urban waste upcycling to a recyclable solid acid catalyst for converting levulinic acid platform molecules into high-value products. *Biofuel Research Journal, 10*(4), 1989-1998. https://doi.org/10.18331/BRJ2023.10.4.5

Costa, B. E. B., da Silva, A. O. S., & Meneghetti, S. M. P. (2024). Esterification of levulinic acid with different alcohols using mesoporous stannosilicates as the catalyst. *ACS Omega, 9*(28), 31128-31135. https://doi.org/10.1021/acsomega.4c04598

Enumula, S. S., Gurram, V. R. B., Chada, R. R., Burri, D. R., & Kamaraju, S. R. R. (2017). Clean synthesis of alkyl levulinates from levulinic acid over one-pot synthesised WO3-SBA-16 catalyst. *Journal of Molecular Catalysis A: Chemical, 426*, 30-38. https://doi.org/10.1016/j.molcata.2016.10.032

Faraguna, F., Racar, M., & Jukić, A. (2019). Test method for determination of different biodiesels (fatty acid alkyl esters) content in diesel fuel using FTIR-ATR. *Renewable Energy, 133*, 1231-1235. https://doi.org/10.1016/j.renene.2018.09.010

Gautam, P., Barman, S., & Ali, A. (2022). A comparative study on the performance of acid catalysts in the synthesis of levulinate ester using biomass-derived levulinic acid: A review. *Biofuels, Bioproducts and Biorefining, 16*(4), 1095-1115. https://doi.org/10.1002/bbb.2351

Gielen, D., Boshell, F., Saygin, D., Bazilian, M. D., Wagner, N., & Gorini, R. (2019). The role of renewable energy in the global energy transformation. *Energy Strategy Reviews, 24*, 38-50. https://doi.org/10.1016/j.esr.2019.01.006

Guo, T., Qiu, M., & Qi, X. (2019). Selective conversion of biomass-derived levulinic acid to ethyl levulinate catalysed by metal organic framework (MOF)-supported polyoxometalates. *Applied Catalysis A: General, 572*, 168-175. https://doi.org/10.1016/j.apcata.2019.01.004

Kothe, V., Melfi, D. T., dos Santos, K. C., Corazza, M. L., & Ramos, L. P. (2020). Thermodynamic analysis, experimental and kinetic modelling of levulinic acid esterification with ethanol at supercritical conditions. *Fuel, 260*, Article 116376. https://doi.org/10.1016/j.fuel.2019.116376

Krishnan, S. G., Pua, F. L., & Fan, Z. (2023). Effect of chemical pre-treatment on the catalytic performance of oil palm EFB fibre-supported magnetic acid catalyst. *Sustainability, 15*(11), Article 8637. https://doi.org/10.1016/j.matpr.2020.01.513

Krishnan, S. G., Pua, F. L., & Jaafar, S. N. S. (2020). Synthesis and characterisation of a local biomass-supported magnetic catalyst for esterification reaction. *Materials Today: Proceedings, 31*, 161-165. https://doi.org/10.1016/j.matpr.2020.01.513

Krishnan, S. G., Pua, F. L., & Zhang, F. (2022). Oil palm empty fruit bunch-derived microcrystalline cellulose-supported magnetic acid catalyst for esterification reaction: An optimisation study. *Energy Conversion and Management: X, 13*, Article 100159. https://doi.org/10.1016/j.ecmx.2021.100159

Kumaravel, S., Thiripuranthagan, S., Radhakrishnan, R., Erusappan, E., Durai, M., Devarajan, A., & Mukannan, A. (2019). Liquid phase esterification of levulinic acid into ethyl levulinate over sulphobenzylated nanoporous Al-SBA-15 catalyst. *Journal of Nanoscience and Nanotechnology, 19*(11), 6965-6977. https://doi.org/10.1166/jnn.2019.16637

Li, N., Jiang, S., Liu, Z. Y., Guan, X. X., & Zheng, X. C. (2019). Preparation and catalytic performance of loofah sponge-derived carbon sulfonic acid for the conversion of levulinic acid to ethyl levulinate. *Catalysis Communications, 121*, 11-14. https://doi.org/10.1016/j.catcom.2018.12.007

Liu, X., Yang, W., Zhang, Q., Li, C., & Wu, H. (2020). Current approaches to alkyl levulinates via efficient valorisation of biomass derivatives. *Frontiers in Chemistry, 8*, Article 794. https://doi.org/10.3389/fchem.2020.00794

Martínez Aguilar, M., Duret, X., Ghislain, T., Minh, D. P., Nzihou, A., & Lavoie, J. M. (2020). A simple process to produce fuel additives using residual lignocellulosic biomass. *Fuel, 264*, Article 116702. https://doi.org/10.1016/j.fuel.2019.116702

Nandiwale, K. Y., Sonar, S. K., Niphadkar, P. S., Joshi, P. N., Deshpande, S. S., Patil, V. S., & Bokade, V. V. (2013). Catalytic upgrading of renewable levulinic acid to ethyl levulinate biodiesel using dodecatungstophosphoric acid supported on desilicated H-ZSM-5 as a catalyst. *Applied Catalysis A: General, 460-461*, 90-98. https://doi.org/10.1016/j.apcata.2013.04.024

Nelson Appaturi, J., Andas, J., Ma, Y.-K., Lee Phoon, B., Muazu Batagarawa, S., Khoerunnisa, F., Hazwan Hussin, M., & Ng, E.-P. (2022). Recent advances in heterogeneous catalysts for the synthesis of alkyl levulinate biofuel additives from renewable levulinic acid: A comprehensive review. *Fuel, 323*, Article 124362. https://doi.org/10.1016/j.fuel.2022.124362

Nindya, C. C. S., Anggara, D. R., Nuryoto, & Teguh, K. (2020). Esterification of glycerol (byproduct in biodiesel production) with oleic acid using mordenite natural zeolite as catalyst: Study of reaction temperature and catalyst loading effect. *IOP Conference Series: Materials Science and Engineering, 909*, Article 012001. https://doi.org/10.1088/1757-899X/909/1/012001

Ogino, I., Suzuki, Y., & Mukai, S. R. (2018). Esterification of levulinic acid with ethanol catalysed by sulfonated carbon catalysts: Promotional effects of additional functional groups. *Catalysis Today, 314*, 62-69.

Patel, A., & Dave, R. (2025). Sugarcane bagasse, a next-generation biomass-derived catalytic material for synthesis of biofuel additives, levulinate esters: Process optimisation and kinetic investigation. *Next Materials, 9*, Article 100979. https://doi.org/10.1016/j.nxmate.2025.100979

Peng, L., Li, H., Xi, L., Chen, K., & Chen, H. (2014). Facile and efficient conversion of furfuryl alcohol into n-butyl levulinate catalysed by extremely low acid concentration. *BioResources, 9*(3), 3825-3834. https://doi.org/10.15376/biores.9.3.3825-3834

Saperi, N. Q., Hassan, A. H., Zainol, M. M., Asmadi, M., Rafizan, A., Daud, M., Yusof, M. Y., & Anggoro, D. D. (2024). Catalytic reaction study of levulinic acid esterification to ethyl levulinate using modified carbon catalyst and acidic DES. *Malaysian Journal of Analytical Sciences, 28*, 724-736.

Shestakova, P., Popova, M., Szegedi, Á., Lazarova, H., Nga Luong, T. K., Trendafilova, I., Mihály, J., & Parac-Vogt, T. N. (2021). Hybrid catalyst with combined Lewis and Brønsted acidity based on ZrIV-substituted polyoxometalate grafted on mesoporous MCM-41 silica for esterification of renewable levulinic acid. *Microporous and Mesoporous Materials, 323*, Article 111203. https://doi.org/10.1016/j.micromeso.2021.111203

Signoretto, M., Taghavi, S., Ghedini, E., & Menegazzo, F. (2019). Catalytic production of levulinic acid (LA) from actual biomass. *Molecules, 24*(15), Article 2760. https://doi.org/10.3390/molecules24152760

Sušjenka, M., Prašnikar, F., Jakovljević Kovač, M., Molnar, M., Fernandes, L., Nunes, A. V. M., Duarte, A. R. C., & Zakrzewska, M. E. (2024). A green chemistry approach to catalytic synthesis of ethyl levulinate. *Catalysts, 14*(12), Article 842. https://doi.org/10.3390/catal14120842

Thangaraj, B., Solomon, P. R., Muniyandi, B., Ranganathan, S., & Lin, L. (2019). Catalysis in biodiesel production: A review. *Clean Energy, 3*(1), 2-23. https://doi.org/10.1093/ce/zky020

Trombettoni, V., Bianchi, L., Zupanic, A., Porciello, A., Cuomo, M., Piermatti, O., Marrocchi, A., & Vaccaro, L. (2017). Efficient catalytic upgrading of levulinic acid into alkyl levulinates by resin-supported acids and flow reactors. *Catalysts, 7*(8), Article 235. https://doi.org/10.3390/catal7080235

Trombettoni, V., Lanari, D., Prinsen, P., Luque, R., Marrocchi, A., & Vaccaro, L. (2018). Recent advances in sulfonated resin catalysts for efficient biodiesel and bio-derived additives production. *Progress in Energy and Combustion Science, 65*, 136-162. https://doi.org/10.1016/j.pecs.2017.11.001

Wang, H., Lu, Y., Liu, H., Yin, Y., & Liang, J. (2020). Preparation and application of magnetic nano-solid acid catalyst Fe3O4-PDA-SO3H. *Energies, 13*(6), Article 1484. https://doi.org/10.3390/en13061484

Yan, L., Yao, Q., & Fu, Y. (2017). Conversion of levulinic acid and alkyl levulinates into biofuels and high-value chemicals. *Green Chemistry, 19*(23), 5527-5547. https://doi.org/10.1039/C7GC02503C

Zainol, M. M., Asmadi, M., Iskandar, P., Wan Ahmad, W. A. N., Amin, N. A. S., & Hoe, T. T. (2021). Ethyl levulinate synthesis from biomass derivative chemicals using iron doped sulfonated carbon cryogel catalyst. *Journal of Cleaner Production, 281*, Article 124686. https://doi.org/10.1016/j.jclepro.2020.124686

Zhang, H., Li, H., Hu, Y., Venkateswara Rao, K. T., Xu, C., & Yang, S. (2019). Advances in production of bio-based ester fuels with heterogeneous bifunctional catalysts. *Renewable and Sustainable Energy Reviews, 114*, Article 109296. https://doi.org/10.1016/j.rser.2019.109296

Zhao, W., Ding, H., Zhu, J., Liu, X., Xu, Q., & Yin, D. (2020). Esterification of levulinic acid into n-butyl levulinate catalysed by sulfonic acid-functionalised lignin-montmorillonite complex. *Journal of Bioresources and Bioproducts, 5*(4), 291-299. https://doi.org/10.1016/j.jobab.2020.10.008

Zhou, S., Liu, Y., Zhang, Y., Liu, Z., Wu, Y., & Liu, X. (2025). Organic–inorganic hybrid solid acid catalyst supported on titanium nanotubes for efficient synthesis of n-butyl levulinate. *Carbon Resources Conversion*, Article 100395. https://doi.org/10.1016/j.crcon.2025.100395